communications
materials

ARTICLE

Check for updates

https://doi.org/10.1038/s43246-023-00427-7 OPEN

Exciton formation dynamics at the SiO_2/Si interface

Sergio Revuelta[1] & Enrique Cánovas[1]✉

Excitons can operate as carriers for energy transduction in optoelectronics, and engineering their dynamics is of great interest. Here, we employ time-resolved terahertz spectroscopy to analyze exciton formation dynamics as a function of temperature for a (100) N-type silicon substrate passivated by native SiO_2. By analyzing the frequency-resolved complex conductivity as a function of temperature we resolve the photophysics for the formation of free carriers into excitons. Notably, we observe a relatively long-lived ~300 ps transient population of free carriers at temperatures well below the Mott transition (4 K). We rationalize this by transient photophysics at the SiO_2/N-type-Si surface, where holes localize and release under high injection conditions due to a transient surface photovoltage effect. We believe our results have implications for the design of excitonic-based electronic applications operating at cryogenic temperatures and accessed optically.

[1]IMDEA Nanociencia, Campus Universitario de Cantoblanco, Madrid, Spain. ✉email: enrique.canovas@imdea.org

Excitons are the main photogenerated species in a plethora of semiconductor systems and their nanostructures, and then, they are critical to the function of many applications related with light absorption and emission (as in solar cells and LEDs). In this respect, engineering the dynamics of excitons and their transport, a field that has been referred as "excitonics", is a current topic of interest in optoelectronics[1–4]. Despite being electrically neutral and dominated by Coulombic interactions, excitons can have long lifetimes even in bulk materials (e.g. up to 10 μs in silicon)[5] where they can also be driven and travel long distances under the application of a strain field in a crystal[6–9]. On their motion, excitons also scatter with lattice defects and/or phonons, and they can reach extremely high mobilities at cryogenic temperatures (e.g. three orders of magnitude higher than the free charge-carrier mobility at room temperature (RT) in silicon[10]).

While excitons can be ubiquitous at room temperature in disordered- organic-based semiconductor materials and low dimensional systems[2,11–13], they are rarer to be found in single crystalline inorganic materials where excitons are generally dissociated right after photon absorption into free electron-hole pairs due to their typically reduced exciton binding energies (within k_BT). However, this simplified picture at room temperature breaks down when the temperature of the system is reduced, then the semiconductor could exhibit different phases varying from a metallic free charge-carrier plasma at high temperature to an insulating exciton gas at lower temperatures, a crossover known as the Mott transition[14–16]. When temperature is even lower and the density of charge carriers is high enough, the exciton gas can undergo a transformation into a plasma-like liquid-phase in the form of electron-hole droplets (EHD)[17–20]. All these phase transitions are not only determined by the temperature of the system, but also by charge-carrier and exciton concentrations[20–22].

The analysis of exciton formation has been historically inferred from photoluminescence (PL) measurements. These measurements can quantify exciton formation by monitoring the near band-edge excitonic radiative recombination of a given sample as a function of injection level and temperature[23–26]. A potential drawback of this approach is that the signal of interest might spectrally overlap with other non-excitonic background signals that can be as well functions of temperature and carrier density (as e.g. the band edge absorption onset and/or the occupation of near band-edge shallow levels). As an alternative, time-resolved terahertz spectroscopy (TRTS) represents an appealing approach. The TRTS technique allows determining the time-resolved frequency-resolved complex photoconductivity in the THz region[27–29] (where $1\,\mathrm{THz} = 4\,\mathrm{meV} = 33\,\mathrm{cm}^{-1}$), from this data one can spectrally distinguish the Drude-like fingerprint of free carriers[30,31] and the Lorentzian-like fingerprint for excitons[32–37]. The strength of this approach to disentangling e-h and excitonic contributions has been already illustrated in several TRTS studies analyzing the Mott transition in gallium arsenide[25,38,39], germanium[34] or silicon[33,35,36]. However, most of these works have primarily focus on analyzing quasi-steady-state bulk-like photo-physics as a function of injection level and temperature. In this case, the work is less abundant on analyzing transient bulk-like exciton dynamics[33,36], and to our knowledge non-existent regarding transient photo-induced exciton dynamics near the surface of the bulk crystal.

Here we analyze TRTS transient exciton formation dynamics as a function of temperature and injection level near the surface of a N-type silicon wafer with <100> orientation, which is natively passivated by silicon oxide (SiO_2 thickness ranges between 1.6 and 4 nm[40,41]). In order to monitor exciton dynamics at the SiO_2/silicon surface we photoexcite the sample with a pump beam centered at 387.5 nm, which defines a penetration depth for the photo-generated carriers of ~80 nm[42]. Our main finding when exploring exciton formation as a function of temperature is that we resolve by TRTS a transient population of free electrons near the silicon surface even at temperatures well below the Mott transition. The transient population of free carriers represent 100% of the photo-species right after photon absorption and condensate into bound excitons fully on a non-negligible time scale of ~300 ps at 4 K. We rationalize our results due to a transient localization and release of holes from the Si/SiO_2 interface. The transient delocalization of holes towards the bulk silicon crystal is induced by a flattening of the near surface depletion region induced by the photo-excitation. The demonstration of optically-pump induced free carriers lasting few hundreds ps in silicon well below the Mott transition might have positive implications for silicon-based devices aiming at exploiting optically pumped free carrier dynamics operating at cryogenic temperatures.

Results and discussion

Observation of a photoconductivity collapse at low temperatures. We have characterized by TRTS a 0.5 mm thick N-type float zone silicon wafer with <100> orientation and native oxide passivation (SiO_2) (Sigma-Aldrich ID: 646687, resistivity range from 100 to 3000 Ω cm that correspond to an electron density between 1×10^{12} and $5 \times 10^{13}\,\mathrm{cm}^{-3}$). Figure 1a shows the time resolved optical pump-terahertz probe (OPTP) dynamics for the real component of the averaged photoconductivity [$Re[\Delta\sigma(t)] \sim \Delta T(t)/T$] at the maximum peak of the terahertz probe in the time-domain (see Supplementary Fig. 1 and Supplementary Discussion 1) and using an optical pump centered at 387.5 nm and at a fluence of 1.03 μJ cm^{-2}. The data reveal the OPTP traces in a 1 ns time window and their evolution at different temperatures ranging from 300 to 4 K. The line shape for the recorded dynamics over the probed 1 ns window show a non-trivial behavior, with a change in both amplitude and line shape as a function of temperature. Later in the manuscript we will discuss in detail about the evolution in temperature of the recorded line-shapes, for the moment, we will focus our discussion on the amplitude dependence of the TRTS photoconductivity shown in Fig. 1a and its different behavior at different pump-probe delays. Figure 1b aims at summarizing this complex evolution by plotting the real photoconductivity amplitude at two different pump-probe delays for the set of analyzed temperatures (see Supplementary Fig. 2 for the complete set of dynamics). At early pump probe delays (i.e., 10 ps in Fig. 1b open symbols) the optical pump-THz probe (OPTP) amplitude has an initial increase between 300 a ~ 230 K which is consistent with a reduction of phonon-carrier scattering[43,44] for the free charge carriers generated upon above gap silicon photoexcitation. However, below ~230 K the photoconductivity of the generated photo-species remains barely constant till 4 K. This behavior was highly unexpected and indicates that the photogenerated species at early pump-probe delays are barely affected by the lattice temperature. On the other hand, the OPTP response as a function of temperature at late pump probe delays shows a different behavior (1 ns in Fig. 1b filled symbols). While in this case we also observe an initial rise in photoconductivity between 300 a ~ 230 K which origin is expected to match with the one suggested at early pump-probe delays (reduction of phonon scattering), this rise is followed by a noticeable decrease in amplitude as the temperature approaches a temperature of 4 K. A decrease in TRTS signal was indeed expected and is likely associated with a reduction in free carrier concentration induced by the formation of photoinduced free charge carriers into excitons[33,35,36].

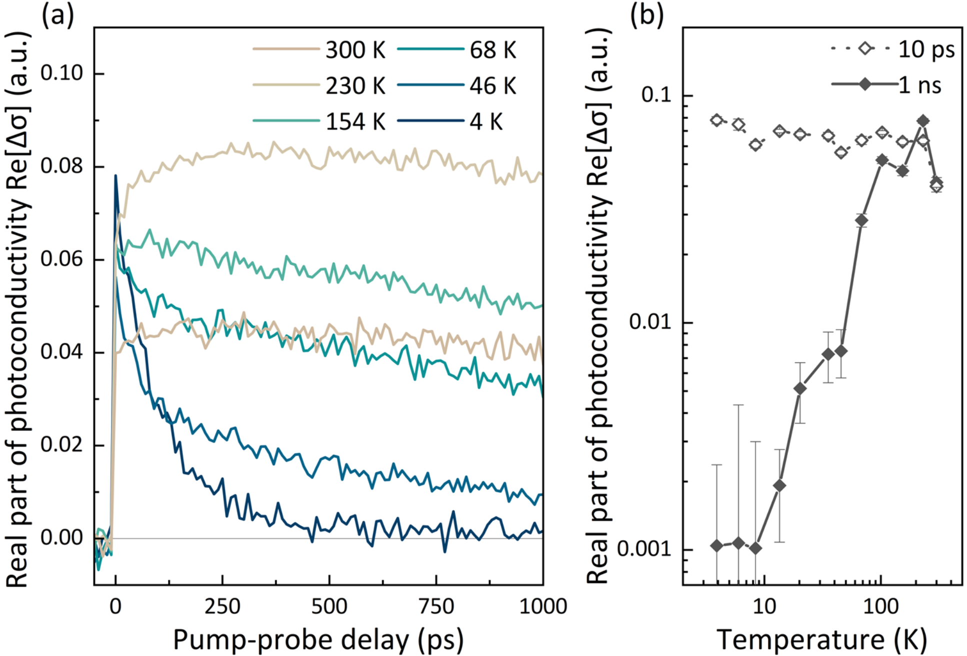

Fig. 1 Real photoconductivity dynamics of silicon as function of temperature. a Time resolved real part of the photoconductivity at as a function of temperature at a fluence of 1.03 μJ cm^{-2}. **b** Amplitude for the real part of the photoconductivity obtained from OPTP data at pump-probe delays of 10 ps (open symbols) and 1 ns (filled symbols). The error bars represent the standard deviation from multiples scans.

Evidence of exciton formation and long-lived free carriers well below the Mott transition. To better understand the nature of these two distinct temperature-dependent behaviors as a function of time after excitation we retrieve the frequency-resolved complex photoconductivity at 5 and 290 ps pump-probe delays for the analyzed range of temperatures (see Fig. 2a, b where filled and open symbols indicate the real and imaginary components respectively). Figure 2a shows the temperature dependent data at 5 ps after photo generation. In this case, all the results, independently of temperature, can be properly fitted by the Drude model:

$$\Delta\sigma_{Drude}(\omega) = \frac{\varepsilon_0 \omega_{p,D}^2 \tau_D}{1 - i\tau_D \omega} \quad (1)$$

Where ε_0 is the vacuum dielectric constant, ω is the angular frequency, τ_D is the scattering time of the free carriers and $\omega_{p,D}$ is the drude plasma frequency. The best fits to de model (following Eq. 1) are given in Fig. 2a by black solid and dashed lines for the real and imaginary parts respectively. The adequate modeling to the Drude model, characterized by a decreasing real and increasing imaginary components (both positive) as a function of frequency for the photoconductivity (solid lines in Fig. 2c), imply that we are probing free delocalized charge carriers at early pump probe delays. These results demonstrate unambiguously the presence of free charge carriers at early times after photoexcitation even well below the onset for the transition to the coexisting electron-hole droplets and excitons expected to happen at ~ 25 K under the injection conditions employed (~ 1×10^{18} cm^{-3}[45], see Fig. 2d).

In contrast, at 290 ps after photoexcitation (see Fig. 2b) we observe that the evolution of the frequency resolved complex conductivity as a function of temperature cannot be fitted by a simple Drude model. Rather there is a clear transition from a Drude-only to a Lorentz-only line shape in the frequency resolved complex photoconductivity when transitioning from high to low temperatures. The Lorentzian-like line shape feature (filled contours in Fig. 2c) was expected as it describes the presence of a bound state centered at ω_0 and is consistent with the presence of excitons in the probed terahertz window[37]. The Lorentz function is given by[27]:

$$\Delta\sigma_{Lorentz} = \frac{\varepsilon_0 \omega_{p,L}^2 \tau_L}{1 - i\tau_L \omega + i\tau_L \omega_0^2/\omega} \quad (2)$$

Where ω_0 is the resonance frequency linked here with the exciton binding energy, τ_L is the inverse of the phenomenological exciton damping constant ($\gamma_L = \tau_L^{-1}$) and $\omega_{p,L}$ is the plasma frequency from the Lorentz model from which the exciton density, N_{exc}, can be retrieved as $\omega_{p,L}^2 = N_{exc} e^2/\varepsilon_0 \mu$, where μ is the exciton effective mass[46]. Employing a linear superposition of Drude+Lorentz fits in Fig. 2b, where the center of the Lorentzian fit was fixed at silicon´s exciton binding energy $E_b = \hbar\omega_0 = 14.7$ meV[47] ($\omega_0 \sim 2.23 \times 10^{13}$ Hz), we can perform appropriate modeling of the data at all temperatures. Note here that in the first approximation we have neglected the eventual fingerprint in our THz window of the contribution of excitons droplets, which could show another resonance centered at larger energies of ~35 meV[36,45] for temperatures below ~25 K.

From the Drude and Drude+Lorentz fits described above we can estimate the ratio of free charge-carriers/excitons as a function of temperature for both pump-probe delays from the retrieved plasma frequencies (see Supplementary Fig. 3). As summarized in Fig. 2e, the yield of free carriers at early pump probe delays is unity independently of temperature (see green inverted triangles). To make this estimate we have considered the known variation of optical density at 387.5 nm vs temperature[48], see Supplementary Discussion 2 for details. For the case of late pump probe delays, we have obtained the free carrier yield through the Mahan relationship[39,49], obtaining a reasonable match between model and experiment with no fitting parameters (see blue open triangles in Fig. 2e, see Supplementary Discussion 3 and Supplementary Fig. 4 for details). In conclusion, Fig. 2e illustrates that at early pump probe delays we are photo-

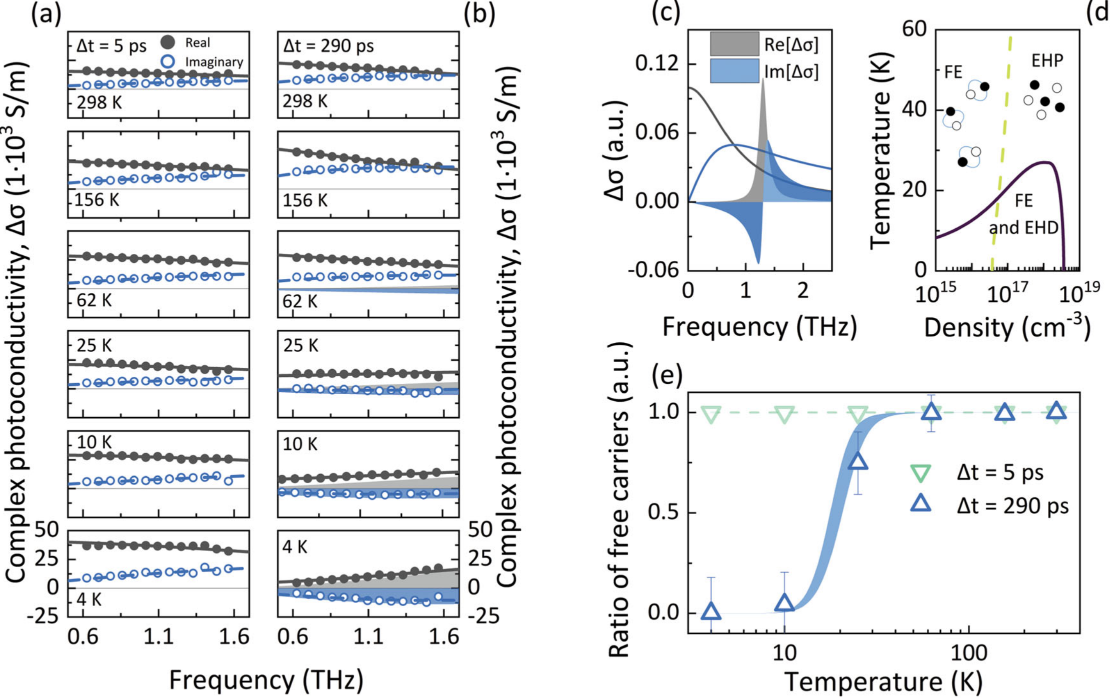

Fig. 2 Exciton formation in silicon. a, **b** Frequency-resolved complex photoconductivity at pump-probe delays of 5 **a** and 290 ps **b** for the indicated temperatures at a fluence of 10.3 μJ cm^{-2}. Black and open symbols refer to the real and imaginary components of the complex photoconductivity respectively. Solid and dashed lines are best fits according to Drude (5 ps) and Drude + Lorentz (290 ps) models. Shadow contours represent the Lorentz contribution to the best-obtained fit. **c** Sketch illustrating the expected lineshapes from the response of free carriers and excitons in the THz region; Solid lines indicate the complex photoconductivity of free carriers following Drude model and filled contours represent the spectral fingerprint of excitons with the Lorentz model. **d** Sketch illustrating the density-temperature phase diagram in silicon. EHP, FE, and EHD refers to electron-hole plasma, free excitons and electron-hole droplets respectively. **e** Ratio of free carriers at 5 (green inverted triangles) and 290 ps (blue triangles) as function of temperature. The dashed line is a guide to the eye while the solid line indicates the model described by the Saha equation for the employed injection level (2.5×10^{18} cm^{-3} and considering deviations of 50% to that injection level). Errors of the free carrier ratio at 290 ps were calculated through the standard deviation of the employed models to the experimental raw data.

generating free charge carriers with unity quantum yield even at temperatures well below excitons are expected to fully populate the samples in steady state conditions. The formation of these photogenerated free carriers into excitons occurs approximately in ~300 ps, an aspect that is further validated from the analysis done as a function pump-probe delay for the trace at 4 K (see Supplementary Fig. 5 in the SI). Below we further interrogate the nature of this signal and propose an explanation about its origin.

Holes trapped near the surface related with the exciton formation. Our initial hypothesis is that the delayed generation of excitons and the persistence of free carriers even below the Mott transition can be explained if one carrier type (e.g. the holes) is localized temporarily near the surface and released within the monitored ~300 ps timescale. A surface related process is supported by the fact that measurements done with an excitation of 775 nm (penetration depth of ~10 μm[50]) with the same photon flux do not show the slow growth after photoexcitation resolved at 387.5 nm (penetration depth of ~80 nm[50]). For 775 nm excitation, OPTP dynamics represent primarily free charge carriers populating the bulk of the crystal, and in this case we observe that the slow rise resolved in the dynamics is not present over the same probed temporal window (see Supplementary Fig. 6). The localization and release hypothesis is indeed consistent with the energetics at the SiO_2/Si interface for our sample, where hole localization at the SiO_2/Si interface for a N-type silicon substrate is expected[6,51,52] (Fig. 3a). Note that under our excitation conditions (80 nm penetration depth), all photo-generated charge carriers are expected to be within the width of the space charge region for this given surface (see Supplementary Discussion 4)[53,54]. In order to check the hypothesis given above, we focus our attention on the eventual emergence of a signal linked to the holes in the TRTS data as a function of pump probe delays. As the photoconductivity is given by the sum of electron and hole conductivities $\Delta\sigma = \Delta\sigma_e + \Delta\sigma_h$, if our hypothesis is true, and the localization of holes near the surface kills their conductivity temporarily, we should be able to resolve this feature in TRTS data by resolving a rise in the monitored dynamics as a function of time after photoexcitation.

We start our analysis by plotting in Fig. 3b the monitored carrier dynamics $Re[\Delta\sigma(t)]$ as function of pump-probe delay for a set of fluences ranging from 0.14 to 3.03 μJ cm^{-2} at room temperature. The dynamics are very singular; For fluences below 1.35 μJ cm^{-2} we observe that dynamics are monophasic and flat over our time window, revealing charge carriers which are long lived and do not experience any recombination. Interestingly, above 1.35 μJ cm^{-2} we observed that dynamics become bi-phasic, with an instant rise that is followed by a rather slow one that lasts ~300 ps. The change in dynamics above ~1.35 μJ cm^{-2} might indeed be consistent with the eventual release of holes from the surface as a function of photon flux. Under the scenario described and illustrated in Fig. 3a, at low fluences we will have that photogenerated charge carriers Δn and Δp are below p_o (i.e., hole density at the surface as illustrated in Fig. 3a) and hence TRTS data should reveal only the minority carrier contribution to the photoconductivity, in this case electrons for N-type substrate

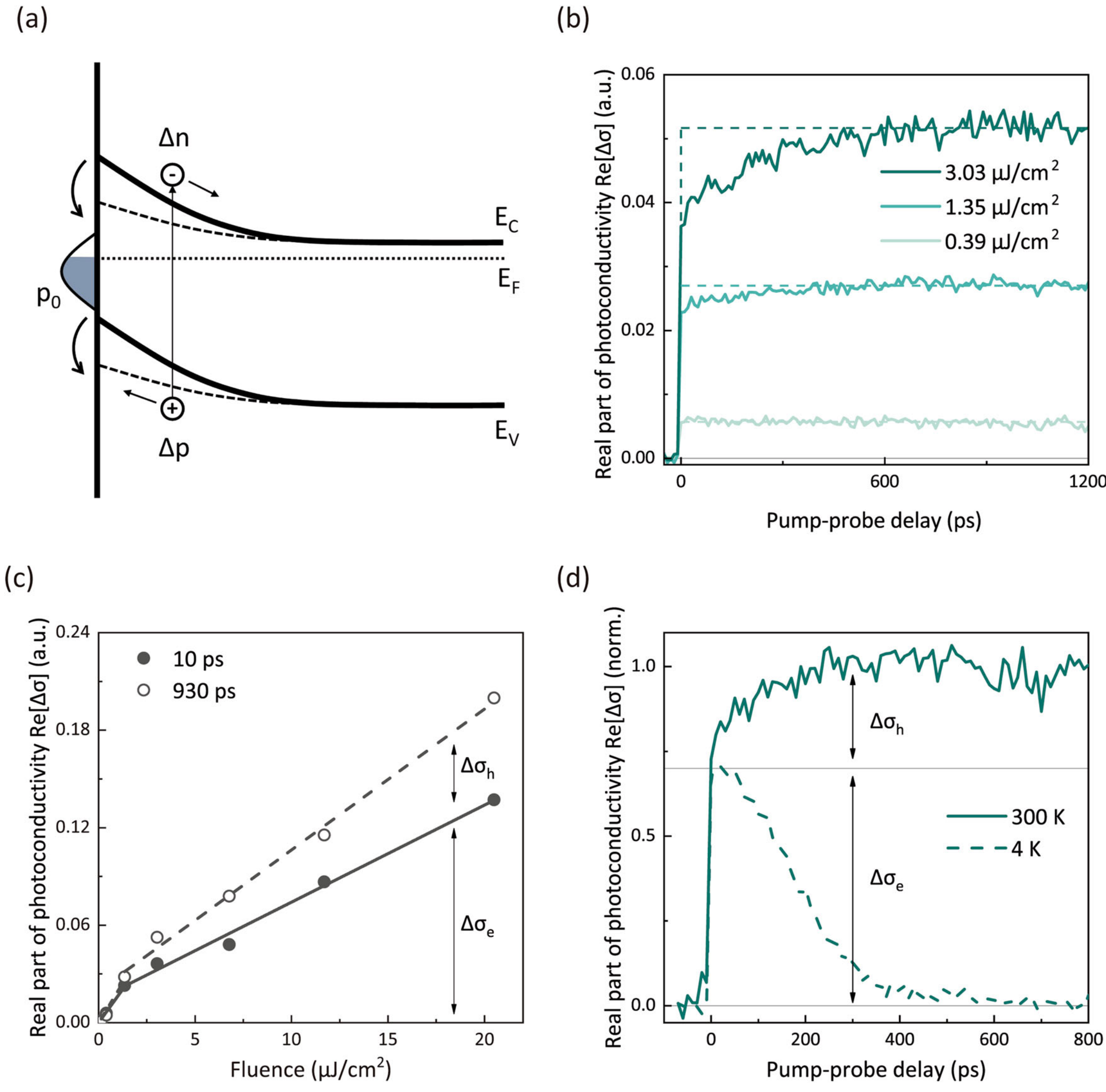

Fig. 3 Effect of the hole's localization near the surface. a A sketch for a SiO_2/N-type-Si surface under illumination. Upon illumination electrons (Δn) and holes (Δp) are generated across the bandgap, with the latter being localized near the surface. The light induces a SPV effect (dashed lines) that will flatten the bands under high injection conditions. **b** Real photoconductivity at RT at different fluences as indicated. **c** Amplitude for the real part of photoconductivity from OPTP data as function of fluence at two different pump-probe delays of 10 ps (filled symbols) and 930 ps (open symbols). Lines show the linear tendency at early (solid line) and late pump probe delays (dashed line); the relative amplitudes for both at any fluence above ~1.35 μJ cm^{-2} reveal the contribution of electrons ($\Delta\sigma_e$) and holes ($\Delta\sigma_h$) to the monitored photoconductivity. **d** Transient OPTP photoconductivity showing a correlation between the rise at 300 K and the decay in dynamics at 4 K. Horizontal line refers the initial 0.7 amplitude when compared with the one at the plateau.

(P-type surface). For fluences above ~1.35 μJ cm^{-2}, we enter the high injection regime (i.e. Δn,Δp are both well above p_o) and then the TRTS signal should show both carriers types that will diffuse in an ambipolar fashion (in agreement with a previous work of our group[31]). Under the energetics depicted in Fig. 3b, with injection above ~1.35 μJ cm^{-2} a surface photovoltage effect (SPV) will be generated, flattening the bands of the space charge region, and triggering the release of holes from the surface. If this scenario applies, the biphasic signals should be purely related with electrons at early pump delays $Re[\Delta\sigma]= \Delta N\, e\, \mu_e$, while at late pump-probe delays the signal should give us information about the real photoconductivity produced by the contribution of both carrier types, electrons and holes, $\mathrm{Re}[\Delta\sigma] = \Delta \mathrm{N}\, e(\mu_e + \mu_h)$. In fact, this is precisely what we observe; in Fig. 3c we illustrate the TRTS amplitude at two different pump-probe delays of 10 and 930 ps for a wide range of fluences (see Supplementary Fig. 7 for all the traces). The initial signal at 10 ps represent a 70% of the total amplitude recorded at 1 ns. This figure perfectly matches expectations as the contribution of electrons in silicon photoconductivity is precisely 70% for the analyzed injection levels (a figure obtained from the ratio of the electron and electron+hole sum silicon mobilities, $\mu_e/\mu_e + \mu_h$; see Supplementary Fig. 8 and Supplementary Fig. 9).

Once we have shown that the RT slow rise linked with the monitored bi-phasic dynamics is consistent with hole release from the SiO_2/Si surface, we analyze its eventual correlation with the slow decay signal found at 4 K. We attempt this correlation under the reasonable assumption that, while one could expect changes on the interfacial chemistry at lower temperatures might affect the SPV, qualitatively the energetics sketched in Fig. 3a should also apply at cryogenic temperatures[55]. Notably, Fig. 3d shows that the "slow" rise at RT seem to correlate with the "slow" decay of dynamics at 4 K. This observation strongly supports the validity of our initial hypothesis where the release of holes from

the surface is behind the relatively long-lived transient formation from free carriers into excitons at cryogenic temperatures; the good correlation in the monitored lifetimes even suggest that the time of flattening of the bands in the space charge regions is barely affected by temperature in our sample. Finally, in order to check whether pump fluence had any effect on the monitored dynamics we analyzed dynamics at 4 K. While we reduced the fluence, we did not observe an increasing lifetime induced by resolving only minority carriers by TRTS, we speculate that this could be linked to a reduced threshold of having high injection conditions at lower temperatures. On the other hand, at larger fluences (still moderate ones, $<2 \times 10^{18}$ cm^{-3}) we observed a non-linear behavior that seems to modulate the time of formation into excitons at 4 K; the behavior is complex and a deeper analysis will be done elsewhere (see Supplementary Fig. 10 in the SI).

The persistence of a TRTS transient pump induced population of free charge carriers in silicon at sub ~100 K temperatures was reported previously by another group[33,36]. In this case, the authors rationalized their observations with a retardation in the thermal relaxation time of the hot charge carriers in the system. Our correlation between RT and low temperature dynamics, with the resolution of an emergence of hole signals, and the observed effect of the variations in fluence in the exciton formation time (see Supplementary Fig. 10) do not seem to support the scenario of hot-carrier cooling. Nevertheless, aiming a correlation of our time scale with published results we have scrutinized the literature. While several works have studied the time dependent surface photovoltage (SPV) dynamics in silicon and other materials[51,56,57], most of these works focused on the signal recovery rather than on the rise time of the process (which should be linked to our observable). In general, most of the X-ray studies are either limited in time resolution or have indeed interpreted a measurable slow rise with an artifact on the measurement protocol (assuming a priori that the pump induced flattening of the bands should be instantaneous, i.e. below the ps timescale[53]). In light of our results, we believe this is not the case, and in support of a relatively slow flattening of the space charge region we point out that time resolved second harmonic generation (SHG) studies on TiO_2 and GaAs showed that the flattening can take indeed lifetimes of few 10 s of ps[58,59]. While the timescale measurable would be dependent on the specificity of system under study, in light of our results, we have to conclude here that the ~300 ps lifetime seen here for the emergence of photo-conductivity signal linked to holes at RT relates directly with the time it takes for the flattening of the bands in the space charge region upon above bandgap photon absorption.

Conclusions

In summary, we have measured charge carrier dynamics by time-resolved terahertz spectroscopy as function of temperature in N-type silicon substrate passivated by native SiO_2. From the analysis of the frequency resolved complex conductivity as a function of temperature we neatly resolve the formation of free carriers into excitons in the samples. Notably, we resolve a ~ 300 ps transient population of free carriers at 4 K, a temperature well below the Mott transition. This observable has been attributed to the photo physics at the SiO_2/N-type-Si surface under pump photo-excitation; where holes will localize and release under high injection conditions due to a SPV effect and the concomitant flattening of the energy bands within the space charge region. We believe these results might open new lines of research where transient excitonic formation effects could be eventually engineered and exploited at the surface of bulk semiconductors. Transient phenomena that, in any case, need to be carefully considered in excitonic based optoelectronic applications as they might play a crucial role in determining the yield of exciton formation and annihilation when surface recombination may play a major role.

Methods

Terahertz spectroscopy. The terahertz (THz) radiation is generated via optical rectification in a 1 mm slab of ZnTe crystal cut along the <110> plane using a Ti:Sapphire laser, which provide us pulses centered at 775 nm at 1 KHz with <150 fs of pulse duration. The detection was performed via electro-optical sampling on an identical ZnTe crystal. The optical pump was achieved by doubling the frequency of the fundamental laser with a BBO crystal, obtaining a central wavelength of 387.5 nm. The frequency resolved complex photoconductivity can be inferred by measuring the transmitted THz pulses from the non-excited sample, $T(\omega)$, and from the pump-induced change in the absorption, $\Delta T(\omega,t)$. See Supplementary Fig. 11 for a scheme of the setup used. Under the employed photoexcitation conditions, the penetration depth is silicon is estimated to be ~80 nm[50], much smaller than the thickness of the sample (0.5 mm). This allows us to employ the Tinkham approximation[27,60] from which we can retrieve the frequency-resolved complex photo-conductivity as:

$$\Delta\sigma(\omega, t) = -\frac{1+n}{Z_0 \cdot l}\frac{\Delta T(\omega, t)}{T(\omega)} \quad (3)$$

Where Z_0 is the intrinsic impedance of free space, n is the refractive index of the medium and l is the penetration depth.

Silicon wafer. Crystalline N-type silicon wafer with native SiO_2 passivation layer and <100> orientation was provided by Sigma-Aldrich under the ID: 646687.

Data availability

The authors declare that all relevant data were available in this paper and its supporting information and that data supporting the results of this study are available from corresponding authors upon reasonable request.

Received: 14 August 2023; Accepted: 6 November 2023;
Published online: 15 November 2023

References

1. Regan, E. C. et al. Emerging exciton physics in transition metal dichalcogenide heterobilayers. *Nat. Rev. Mater.* **7**, 778 (2022).
2. Tartakovskii, A. Excitons in 2D Heterostructures. *Nat. Rev. Phys.* **2**, 8 (2020).
3. Wang, H. et al. An excitonic perspective on low-dimensional semiconductors for photocatalysis. *J. Am. Chem. Soc.* **142**, 14007 (2020).
4. Rodin, A., Trushin, M., Carvalho, A. & Castro Neto, A. H. Collective excitations in 2D materials. *Nat. Rev. Phys.* **2**, 524 (2020).
5. Wolfe, J. P. Thermodynamics of excitons in semiconductors. *Phys. Today* **35**, 46 (1982).
6. Kronik, L. & Shapira, Y. Surface photovoltage phenomena: theory, experiment, and applications. *Surf. Sci. Rep.* **37**, 1 (1999).
7. Gourley, P. L. & Wolfe, J. P. Thermodynamics of excitonic molecules in silicon. *Phys. Rev. B* **20**, 3319 (1979).
8. Gourley, P. L. & Wolfe, J. P. Properties of the electron-hole liquid in Si: zero stress to the high-stress limit. *Phys. Rev. B* **24**, 5970 (1981).
9. Aldred, A. T., Lam, D. J., Gourley, P. L. & Wolfe, J. P. Spatial condensation of strain-confined excitons and excitonic molecules into an electron-hole liquid in silicon. *Phys. Rev. Lett.* **40**, 526 (1977).
10. Tamor, M. A. & Wolfe, J. P. Drift and diffusion of free excitons in Si. *Phys. Rev. Lett.* **44**, 1703 (1980).
11. Liu, Y. et al. Room temperature nanocavity laser with interlayer excitons in 2D heterostructures. *Sci. Adv.* **5**, eaav4506 (2023).
12. Zhu, X.-Y., Yang, Q. & Muntwiler, M. Charge-transfer excitons at organic semiconductor surfaces and interfaces. *Acc. Chem. Res.* **42**, 1779 (2009).

13. Mikhnenko, O. V., Blom, P. W. M. & Nguyen, T.-Q. Exciton diffusion in organic semiconductors. *Energy Environ. Sci.* **8**, 1867 (2015).
14. Mott, N. F. Metal-insulator transition. *Rev. Mod. Phys.* **40**, 677 (1968).
15. Zimmermann, R., Kiijmann, K., Kraeft, W. D., Kremp, D. & Ropke, G. Dynamical screening and self-energy of excitons in the electron-hole plasma. *Physica Status Solidi* **90**, 175 (1978).
16. Zimmermann, R. & Stolz, H. The mass action law in two-component fermi systems revisited excitons and electron-hole pairs. *Physica Status Solidi* **131**, 151 (1985).
17. Rothenberg, M. S. Electron–hole droplets in germanium and silicon. *Phys. Today* **26**, 17 (1973).
18. C. Benoit *à la Guillaume, Electron-Hole Droplets in Semiconductors, in Collective Excitations in Solids*, edited by B. Bartolo, **88** (*NATO advanced* science institutes series, Chestnut Hili, 1983), pp. 633–642.
19. Jeffries, C. D. & Keldysh, L. V. Electron-Hole Droplets in *Semiconductors, in* (1983).
20. Rice, T. M. The electron-hole liquid in semiconductors: theoretical aspects. *in Solid State Physics*, edited by H. Ehrenreich, F. Seitz, and D. Turnbull, Vol. 32 (Academic Press, 1978), pp. 1–86.
21. Forchel, A., Laurich, B., Wagner, J., Schmid, W. & Reinecke, T. L. Systematics of electron-hole liquid condensation from studies of silicon with varying uniaxial stress. *Phys. Rev. B* **25**, 2730 (1982).
22. Reinecke, T. L., Lega, M. C. & Ying, S. C. Model of electron-hole droplet condensation in semiconductors. *Phys. Rev. B* **20**, 1562 (1979).
23. Pelant, I. & Valenta, J. Luminescence of excitons. in *Luminescence Spectroscopy of Semiconductors* (Oxford University Press, 2012), pp. 161–204.
24. Kumar, R., Vengurlekar, A. S., Prabhu, S. S., Shah, J. & Pfeiffer, L. N. Picosecond time evolution of free electron-hole pairs into excitons in GaAs quantum wells. *Phys. Rev. B* **54**, 4891 (1996).
25. Amo, A., Martín, M. D., Viña, L., Toropov, A. I. & Zhuravlev, K. S. Photoluminescence dynamics in GAAS along an optically induced mott transition. *J. Appl. Phys.* **101**, 081717 (2007).
26. Kappei, L., Szczytko, J., Morier-Genoud, F. & Deveaud, B. Direct observation of the Mott transition in an optically excited semiconductor quantum well. *Phys. Rev. Lett.* **94**, 147403 (2005).
27. Ulbricht, R., Hendry, E., Shan, J., Heinz, T. F. & Bonn, M. Carrier dynamics in semiconductors studied with time-resolved terahertz spectroscopy. *Rev. Mod. Phys.* **83**, 543 (2011).
28. Kužel, P. & Němec, H. Terahertz spectroscopy of nanomaterials: a close look at charge-carrier transport. *Adv. Opt. Mater.* **8**, 1 (2020).
29. Schmuttenmaer, C. A. Exploring dynamics in the far-infrared with terahertz spectroscopy. *Chem. Rev.* **104**, 1759 (2004).
30. Mics, Z., D'Angio, A., Jensen, S. A., Bonn, M. & Turchinovich, D. Density-dependent electron scattering in photoexcited GaAs in strongly diffusive regime. *Appl. Phys. Lett.* **102**, (2013).
31. Revuelta, S. & Cánovas, E. Contactless determination and parametrization of charge-carrier mobility in silicon as a function of injection level and temperature using time-resolved Terahertz spectroscopy. *Phys. Rev. B* **107**, 085204 (2023).
32. Hendry, E., Koeberg, M. & Bonn, M. Exciton and electron-hole plasma formation dynamics in ZnO. *Phys. Rev. B* **76**, 045214 (2007).
33. Suzuki, T. & R. Shimano, R. Cooling dynamics of photoexcited carriers in Si studied using optical pump and terahertz probe spectroscopy. *Phys. Rev. B Condens. Matter Mater. Phys.* **83**, (2011).
34. Sekiguchi, F. & Shimano, R. Excitonic correlation in the mott crossover regime in Ge. *Phys. Rev. B Condens. Matter Mater. Phys.* **91**, (2015).
35. Suzuki, T. & Shimano, R. Exciton mott transition in Si revealed by terahertz spectroscopy. *Phys. Rev. Lett.* **109**, 1 (2012).
36. Suzuki, T. & Shimano, R. Time-resolved formation of excitons and electron-hole droplets in si studied using terahertz spectroscopy. *Phys. Rev. Lett.* **103**, 1 (2009).
37. Kaindl, R. A., Carnahan, M. A., Hägele, D., Lövenich, R. & Chemla, D. S. Ultrafast terahertz probes of transient conducting and insulating phases in an electron-hole gas. *Nature* **423**, 734 (2003).
38. F. Sekiguchi, C. Kim, H. Akiyama, and R. Shimano, *Exciton Mott Transition in GaAs Studied by Terahertz Spectroscopy, in Ultrafast Phenomena and Nanophotonics XXI*, Vol. 10102 (SPIE, 2017), p. 101020T.
39. Kaindl, R. A., Hägele, D., Carnahan, M. A. & Chemla, D. S. Transient terahertz spectroscopy of excitons and unbound carriers in quasi-two-dimensional electron-hole gases. *Phys. Rev. B Condens. Matter Mater. Phys.* **79**, 1 (2009).
40. Bohling, C. & Sigmund, W. Self-limitation of native oxides explained. *Silicon* **8**, 339 (2016).
41. Alay, J. L. & Hirose, M. The valence band alignment at ultrathin SiO_2/Si interfaces. *J. Appl. Phys.* **81**, 1606 (1997).
42. De Graaf, G. & Wolffenbuttel, R. F. Illumination source identification using a CMOS optical microsystem. *IEEE Trans. Instrum. Meas.* **53**, 238 (2004).
43. Böer, K. W. & Pohl, U. W. *Semiconductor Physics* (2018).
44. Jacoboni, C., Canali, C., Ottaviani, G. & Alberigi Quaranta, A. A review of some charge transport properties of silicon. *Solid State Electron.* **20**, 77 (1977).
45. Navarro, H., Zarate, H. G. & Timusk, T. The far-infrared absorption spectrum of electron-hole drops in silicon. *Solid State Commun* **25**, 1045 (1978).
46. Lipari, N. O. & Baldereschi, A. Energy levels of indirect excitons in semiconductors with degenerate bands. *Phys. Rev. B* **3**, (1971).
47. Shaklee, K. L. & Nahory, R. E. Valley-orbit splitting of free excitons? The absorption edge of Si. *Phys. Rev. Lett.* **24**, 942 (1970).
48. Jellison, G. E. Jr. & Modine, F. A. Optical absorption of silicon between 1.6 and 4.7 EV at elevated temperatures. *Appl Phys Lett* **41**, 180 (1982).
49. Burgos-Caminal, A., Socie, E., Bouduban, M. E. F. & Moser, J. E. Exciton and carrier dynamics in two-dimensional perovskites. *J. Phys. Chem. Lett.* **11**, 7692 (2020).
50. Green, M. A. Self-consistent optical parameters of intrinsic silicon at 300K including temperature coefficients. *Solar Energy Mater. Solar Cells* **92**, 1305 (2008).
51. Kamrla, R. et al. SiO 2/Si(001) studied by time-resolved valence band photoemission at MHz repetition rates: linear and nonlinear excitation of surface photovoltage. *J. Vacuum Sci. Technol. A* **37**, 021101 (2019).
52. Spencer, B. F. et al. Time-resolved surface photovoltage measurements at n-type photovoltaic surfaces: Si(111) and ZnO(1010). *Phys. Rev. B* **88**, 195301 (2013).
53. Widdra, W. et al. Time-resolved core level photoemission: surface photovoltage dynamics of the SiO_2/Si(1 0 0) interface. *Surf Sci* **543**, 87 (2003).
54. Sze, S. M. & Lee, M. K. *Semiconductor Devices: Physics and Technology*, *3rd Edition* (John Wiley & Sons, Inc., 2016).
55. Zhang, H. M., Sakamoto, K., Hansson, G. V. & Uhrberg, R. I. G. High-Temperature Annealing and Surface Photovoltage Shifts on Si(111)7×7. *Phys Rev B* **78**, 35318 (2008).
56. Spencer, B. F. et al. Time-resolved surface photovoltage measurements at n-type photovoltaic surfaces: Si(111) and ZnO($10\bar{1}0$). *Phys. Rev. B Condens. Matter Mater. Phys.* **88**, (2013).
57. Tang, H. et al. Photo-modulated optical and electrical properties of graphene. *Nanophotonics* **11**, 917–940 (2022).
58. Hazama, Y. et al. Revealing solar-cell photovoltage dynamics at the picosecond time scale with time-resolved photoemission spectroscopy. *Phys. Rev. Appl.* **10**, 34056 (2018).
59. Lantz, J. M. & Corn, R. M. Time-resolved optical second harmonic generation measurements of picosecond band flattening processes at single crystal TiO_2 electrodes. *J Phys Chem* **98**, 9387 (1994).
60. Glover, R. E. & Tinkham, M. Conductivity of superconducting films for photon energies between 0.3 and 40kTc. *Phys. Rev.* **108**, 243 (1957).

Acknowledgements

We acknowledge financial support from Grants Nos. PID2019-107808RA-I00, TED2021-129624B-C44 and CNS2022-136203 funded by MCIN/AEI/10.13039/501100011033 and by "NextGenerationEU"/PRTR. IMDEA Nanociencia acknowledges support from the 'Severo Ochoa' Programme for Centres of Excellence in R&D (MINECO, Grant SEV-2016-0686). We also acknowledge financial support from the Comunidad de Madrid through Projects Nos. 2017-T1/AMB-5207 and 2021–5 A/AMB-20942. We acknowledge Prof. Dr. Rodolfo Miranda and Prof. Dr. David Fuertes-Marrón for fruitful discussions about data interpretation and analysis. We also acknowledge Prof. Dr. Reinhold Wannemacher for his assistance with the cryogenic measurements.

Author contributions

S.R. conducted the measurements. E.C. designed and directed the project. S.R. and E.C. contributed to the data analysis, interpretation, and writing the manuscript.

Competing interests

The authors declare no competing interests.

Additional information

Supplementary information The online version contains supplementary material available at https://doi.org/10.1038/s43246-023-00427-7.

Correspondence and requests for materials should be addressed to Enrique Cánovas.

Peer review information *Communications Materials* thanks Takeshi Suzuki and the other, anonymous, reviewer(s) for their contribution to the peer review of this work. Primary Handling Editors: Klaas-Jan Tielrooij and Aldo Isidori. A peer review file is available.

Reprints and permission information is available at http://www.nature.com/reprints

Publisher's note Springer Nature remains neutral with regard to jurisdictional claims in published maps and institutional affiliations.

Open Access This article is licensed under a Creative Commons Attribution 4.0 International License, which permits use, sharing, adaptation, distribution and reproduction in any medium or format, as long as you give appropriate credit to the original author(s) and the source, provide a link to the Creative Commons license, and indicate if changes were made. The images or other third party material in this article are included in the article's Creative Commons license, unless indicated otherwise in a credit line to the material. If material is not included in the article's Creative Commons license and your intended use is not permitted by statutory regulation or exceeds the permitted use, you will need to obtain permission directly from the copyright holder. To view a copy of this license, visit http://creativecommons.org/licenses/by/4.0/.

© The Author(s) 2023